Order online now!

www.rockland.com
tech@rockland.com
+1 484.791.3823

Datasheet for 600-101-196

Apolipoprotein A-I Antibody

Overview

Description:	Anti-Apolipoprotein A-I (GOAT) Antibody - 600-101-196
Item No.:	600-101-196
Size:	1 mg
Applications:	ELISA, IF, IHC, Other, WB
Reactivity:	Mouse
Host Species:	Goat

Product Details

Background:	Anti Apolipoprotein A-I antibody recognizes the gene product of APOA1. Apolipoprotein promotes cholesterol efflux from tissues to the liver for excretion. Apolipoprotein A-I is the major protein component of high density lipoprotein (HDL) in the plasma. Synthesized in the liver and small intestine, it consists of two identical chains of 77 amino acids; an 18-amino acid signal peptide is removed co-translationally and a 6-amino acid propeptide is cleaved post-translationally. Variation in the latter step, in addition to modifications leading to so-called isoforms, is responsible for some of the polymorphism observed. APOA1 is a cofactor for lecithin cholesterolacyltransferase (LCAT) which is responsible for the formation of most plasma cholesteryl esters. The APOA1, APOC3 and APOA4 genes are closely linked in both rat and human genomes. The A-I and A-IV genes are transcribed from the same strand, while the C-III gene is transcribed convergently in relation to A-I. Defects in the apolipoprotein A-1 gene are associated with HDL deficiency and Tangier disease. This antibody is suitable for cardiovascular research.
Synonyms:	goat anti-Apolipoprotein A-I Antibody, goat anti-APOA1 antibody, goat anti-APO-A1 antibody, goat anti-APOA-1 antibody, APOA1/APOC3 fusion gene antibody, Apolipoprotein A I precursor antibody, Apolipoprotein AI antibody, Apolipoprotein of high density lipoprotein antibody, ProapoA-I, Proapolipoprotein A-I
Host Species:	Goat
Clonality:	Polyclonal
Format:	IgG

Target Details

Gene Name:	Apoa1
Reactivity:	Mouse
Immunogen Type:	Native Protein
Immunogen:	apoLipoprotein Type A-I was isolated from mouse plasma by density gradient centrifugation followed by HPLC purification.
Purity/Specificity:	This product has been prepared by immunoaffinity chromatography using immobilized antigens followed by extensive cross-adsorption against other apoLipoproteins and human serum proteins to remove any unwanted specificities. Typically less than 1% cross-reactivity against other types of apoLipoprotein was detected by ELISA against purified standards. This antibody reacts with mouse apoLipoprotein A-I and has negligible cross-reactivity with Type A-II, B, C-I, C-II, C-III, E and J apoLipoproteins. Specific cross-reaction of anti-apoLipoprotein antibodies with antigens from other species has not been determined. Non-specific cross-reaction of anti-apoLipoprotein antibodies with other mouse serum proteins is negligible.
Relevant Links:	• 600-101-196 SDS • UniProtKB - Q00623 • NCBI - NP_033822.2 • GeneID - 11806

Application Details

Suggested Applications:	ELISA, IF, IHC, Other, WB (Based on references)
Application Note:	Anti-apoLipoprotein antibodies have been used for indirect trapping ELISA for quantitation of antigen in serum using a standard curve, for immunoprecipitation and for western blotting for highly sensitive qualitative analysis.
Assay Dilutions:	All assays should be optimized by the user. Recommended dilutions (if any) may be listed below.
ELISA:	1:5,000 - 1:10,000
IHC:	1:250 - 1:500
IP:	1:100
WB:	1:500 - 1:1,000

Formulation

Physical State:	Liquid (sterile filtered)
Concentration:	1.0 mg/mL by UV absorbance at 280 nm

Buffer:	0.125 M Sodium Borate, 0.075 M Sodium Chloride, 0.005 M EDTA, pH 8.0
Preservative:	0.01% (w/v) Sodium Azide
Stabilizer:	None

Shipping & Handling

Shipping Condition:	Wet Ice
Storage Condition:	Store vial at 4° C prior to opening. This product is stable at 4° C as an undiluted liquid. Dilute only prior to immediate use. For extended storage, mix with an equal volume of glycerol, aliquot contents and freeze at -20° C or below. Avoid cycles of freezing and thawing.
Expiration:	Expiration date is one (1) year from date of receipt.

Images

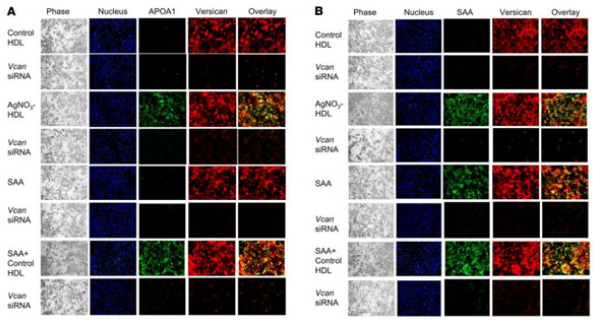

Immunofluorescence Microscopy
Immunofluorescence of Anti-Apolipoprotein AI. Versican colocalizes with HDL isolated from AgNO3-injected mice at the cell surface of 3T3-L1 adipocytes. Free SAA and HDL from PBS- or AgNO3-injected C57BL/6 mice were isolated. Some adipocytes were transfected with siRNA specific for versican (Vcan) for 3 days. After exposure to free SAA (15 µg/mL) and/or these HDL preparations (50 µg protein/mL) for 6 hours, 3T3-L1 adipocytes were fixed in 2% formalin for 5 minutes. After extensively washing, (A) APOA1 and versican were stained using anti-versican (shown in red) and anti-APOA1 (shown in green) antibodies, or (B) SAA and versican were stained using anti-versican (shown in red) and anti-SAA (shown in green) antibodies and photographed by fluorescence microscopy (Nikon Eclipse 80i, original magnification, ×200). Cell nuclei were counterstained with DAPI (blue). Cell morphology was shown by phase-contrast photography (left). Merged fluorescence (overlay) is shown in yellow. Figure 2. PMID: 32970631.

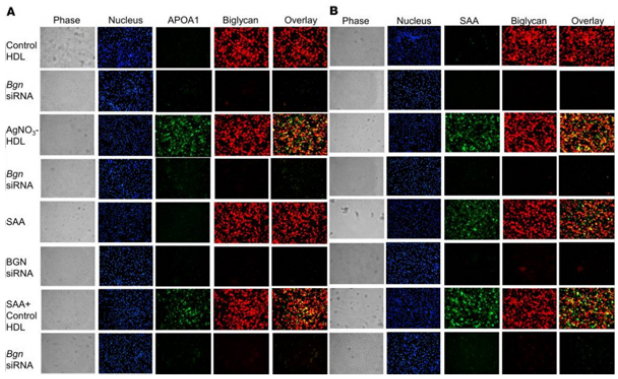

Immunofluorescence Microscopy

Immunofluorescence of Anti-Apolipoprotein AI.
HDL isolated from AgNO3-injected mice colocalizes with biglycan at the cell surface of peritoneal macrophages. HDL from PBS- and AgNO3-injected C57BL/6 mice was isolated. After exposure to these HDL preparations (50 µg protein/mL) for 6 hours, TG-elicited peritoneal macrophages from Saa3–/– were fixed in 2% formalin for 5 minutes (A and B). After extensive washing, (A) APOA1 and biglycan were stained using anti-biglycan (red) and anti-APOA1 (green) antibodies, or (B) SAA and biglycan were stained using anti-biglycan (red) and ant-SAA (green) antibodies and photographed by fluorescence microscopy (Nikon Eclipse 80i, original magnification, ×200). Figure 5. PMID: 32970631.

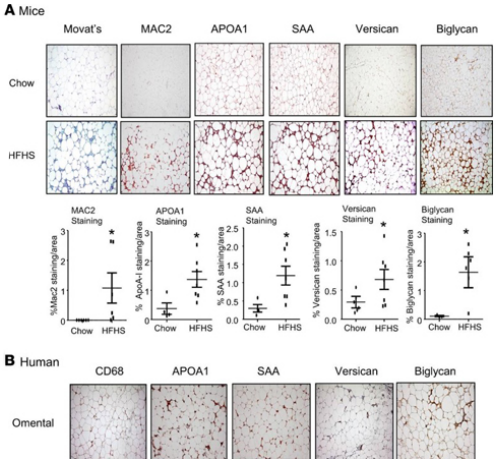

Immunohistochemistry

Immunohistochemistry of Anti-Apolipoprotein AI.
Immunohistochemical staining of versican and biglycan shows a similar distribution with the staining of SAA and APOA1 in the epididymal white adipose tissue from mice fed an HFHS diet and in the omental fat tissue from human obese subjects undergoing gastric bypass surgery. (A) Mice were fed a chow or HFHS diet for 16 weeks, after which adipose tissue was obtained and immunostained with the antibodies shown. Tissues were photographed using microscopy (original magnification, ×60). Quantitation of the immunostaining is shown in the lower panel (n = 5–7, mean ± SEM). *P < 0.001 vs. chow. (B) Omental fat was obtained from gastric bypass patients and immunostained with the antibodies shown. Tissues were photographed using microscopy (original magnification, ×60). The pictures of MAC2, CD68, versican, and biglycan staining are from our previous publication (17); APOA1 and SAA staining were performed on adjacent sections. Figure 1. PMID: 32970631.

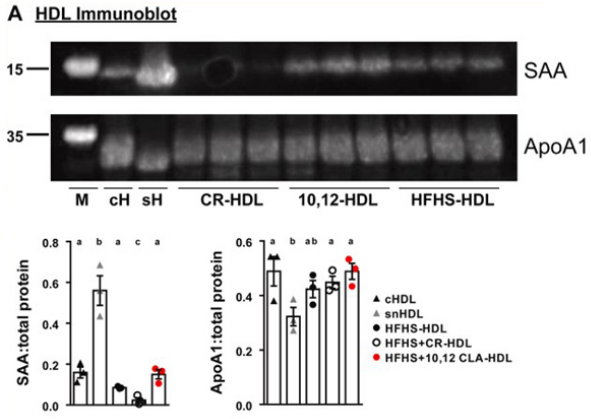

Western Blot

Western Blot of Anti-Apolipoprotein AI.

Proteomics confirmation and hepatic gene expression. A: HDL preparations from the indicated treatment groups were subjected to immunoblot and probed for Saa (marker = 15 kD) and Apoa1 (marker = 35 kD). Densitometry was performed using ImageJ software. Control HDL samples were pooled; n = 3 for treatment groups. Different letters indicate significant differences, assessed using one-way ANOVA with multiple comparisons (Tukey) ($P < 0.05$). cH, control HDL from mice injected with saline; CR-HDL, HDL from mice fed an HFHS diet that were calorically restricted; 10,12-HDL, HDL from mice fed an HFHS diet containing 10,12 CLA; HFHS-HDL, HDL from mice fed an HFHS diet; sH, HDL from mice injected with silver nitrate. B: Liver gene expression was quantified from the indicated treatment groups. n = 8 mice/group, ⍰P < 0.05 from HFHS. Fig. 5. PMID: 35714730.

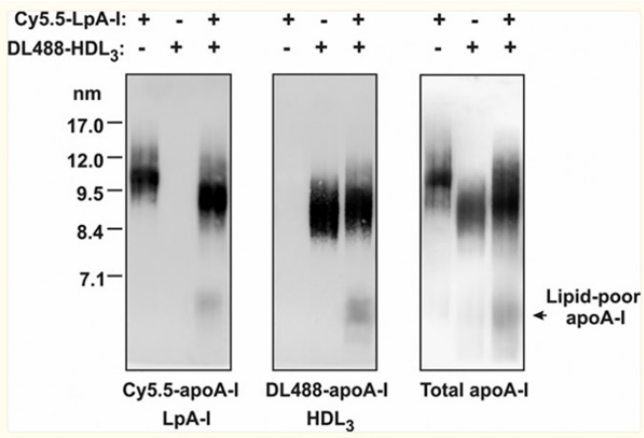

Western Blot

Western Blot of Anti-Apolipoprotein AI.

Lipoprotein particle remodeling is induced by the interaction of nascent LpA-I (apo AI [apolipoprotein AI] containing particles formed by incubating ABCA1 [ATP-binding cassette transporter 1]-expressing cells with apo AI) and HDL3 in vitro. Fluorescently labeled LpA-I (Cy5.5-LpA-I) and HDL3 (DL488-HDL3) were incubated for 1 h at 37°C, final concentration of each lipoprotein was 0.5 mg/mL. Lipoproteins were subjected to nondenaturing polyacrylamide gradient gel electrophoresis. Cy5.5–apo AI (left) and DL488–apo AI (middle) were visualized by fluorescent imaging, apo AI (right) was detected by anti-apo AI antibody. The migration of lipid-poor apo AI is also indicated. HDL indicates high-density lipoprotein. Figure 3. PMID: 32131613.

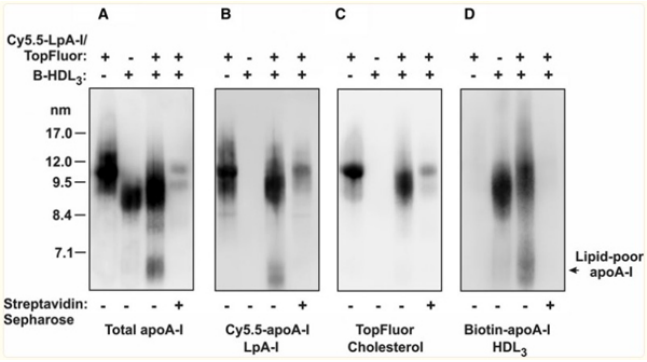

Western Blot

Western Blot of Anti-Apolipoprotein AI.
Cholesterol transfer between nascent LpA-I (apo AI [apolipoprotein AI] containing particles formed by incubating ABCA1 [ATP-binding cassette transporter 1]-expressing cells with apo AI) and HDL3 takes place during particle remodeling in vitro. Cy5.5-LpA-I/TopFluor particles containing TopFluor-cholesterol were incubated with B-HDL3 (biotinylated HDL3) for 1 h at 37°C, final concentration of each lipoprotein was 0.5 mg/mL. Following treatment of the reaction mixtures with Sepharose beads (−) or Streptavidin Sepharose beads (+), lipoproteins remained in the supernatants were separated by nondenaturing polyacrylamide gradient gel electrophoresis. apo AI (A) and biotinylated apo AI (D) were detected with anti-apo AI antibody and NeutrAvidin, respectively. Cy5.5–apo AI (B) and TopFluor-cholesterol (C) were visualized by fluorescent imaging. The position of migration of lipid-poor apo AI is indicated. HDL, high-density lipoprotein. Figure 4. PMID: 32131613.

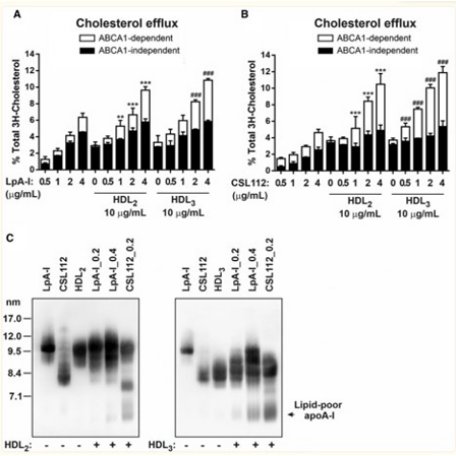

Western Blot

Western Blot of Anti-Apolipoprotein AI.
Small discoidal CSL112 induces more lipid-poor apo AI (apolipoprotein AI) upon incubation with HDL (high-density lipoprotein) compared with the nascent LpA-I (apo AI containing particles formed by incubating ABCA1 [ATP-binding cassette transporter 1]-expressing cells with apo AI). HDL3 or HDL2 (final protein concentration 1 mg/mL) were incubated for 1 h at 37°C in the absence or presence of increasing concentrations of LpA-I or CSL112 (at 0.05, 0.1, 0.2, and 0.4 mg protein/mL). Cholesterol efflux from RAW264.7 macrophages is shown (A and B). Final concentrations of LpA-I (A) or CSL112 (B) in efflux medium were 0.5, 1, 2, and 4 µg protein/mL; HDL3 or HDL2 were at 10 µg protein/mL, as indicated. Data from three independent experiments are shown. Values are presented as mean±SD. ABCA1-dependent efflux: ***P<0.001, **P<0.01 vs HDL2; ### P<0.001 vs HDL3. C, HDL2 or HDL3 (final protein concentration 1 mg/mL) were incubated with LpA-I (0.2 and 0.4 mg/mL final protein concentrations; [LpA_0.2] and [LpA_0.4], respectively) or CSL112 (final protein concentration 0.2 mg/mL; [CSL112_0.2]) for 1 h at 37°C. Lipoproteins were separated by nondenaturing polyacrylamide gradient gel electrophoresis, and apo AI was detected by anti–apo AI antibody. The migration of lipid-poor apo AI is indicated. Figure 6. PMID: 32131613.

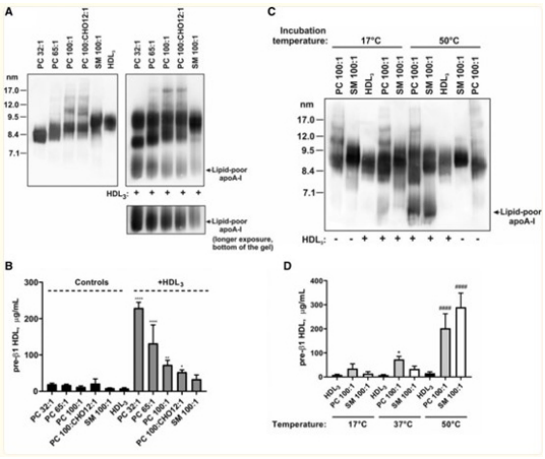

Western Blot

Western Blot of Anti-Apolipoprotein AI. Phospholipid:protein ratio and lipid composition of discoidal HDLs (high-density lipoproteins) impact on interaction with HDL3 and apo AI (apolipoprotein AI) release. HDL3 (final protein concentration 1 mg/mL) was incubated for 1 h with different formulations of reconstituted HDL (final protein concentration 1 mg/mL) as indicated. Lipid-poor apo AI was analyzed either by Western blotting with anti–apo AI antibody following separation of lipoproteins by nondenaturing polyacrylamide gradient gel electrophoresis (A and C) or by pre-β1 HDL ELISA (B and D). Lipoproteins incubated alone in PBS were included as controls. A and B, Incubation at 37°C. C, Incubation at 17°C and 50°C. D, Shown data for incubations of HDL3 with phosphatidylcholine (PC) 100:1 apo AI (gray bars) and sphingomyelin (SM) 100:1 apo AI (white bars) at 17°C, 37°C and 50°C. B and D, Data from three independent experiments are shown. Values are presented as mean±SD. B, Pre-β1: ****P<0.0001, ***P<0.001, **P<0.01, *P<0.05 vs HDL3. D, Pre-β1: ####P<0.0001 and *P<0.05 vs HDL3, for incubations at 50°C and 37°C, respectively. Figure 7. PMID: 32131613.

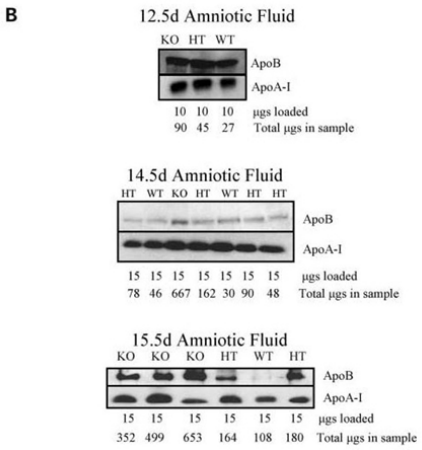

Western Blot

(B) Representative western blots of ApoB and ApoA-I in amniotic fluid at various gestational ages. Equal amounts of total protein were loaded for each sample of a set. The total amount of protein in each sample is also indicated. Fig 3. PMID: 16301212

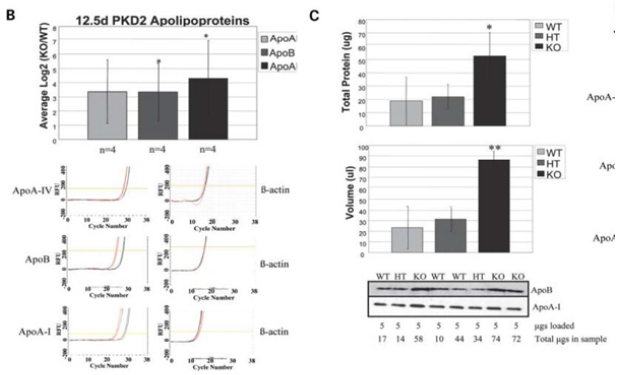

Western Blot

Pkd2−/− mouse placentae have histological and transcriptional alterations similar to those of Pkd1−/− specimens. (A) Representative sections from the labyrinth layer of 14.5 d.p.c. Pkd2+/+ (WT) and Pkd2−/−(KO) placentas stained with H&E and α-laminin. (B) Average Log2(KO/WT) values and representative real-time graphs are shown for Apo genes for littermate pairs of Pkd2−/− (red) and Pkd2+/+ (black) 12.5 d.p.c. placental specimens. Average Log2(KO/WT) values: ApoA-IV = 3.4 ±2.2; ApoB = 3.3 ±2; ApoA-I = 4.3 ±2.7. 'n' indicates the number of pairs of specimens examined with each probe. Apo gene expression levels were normalized to those of β-actin. *P < 0.05 (Paired Student's t -test). (C) Pkd2−/− mice have greater quantities of apolipoproteins in their amniotic fluid. Top: Averages of total protein levels (top) and total volume (bottom) in amniotic fluid samples from 12.5 d.p.c (4WT, 8 HT, 6 KO) specimens. *P < 0.05; **P < 0.001 compared with HT and WT (Student's t-test). Average volumes in µl: WT 23.3 ±19.9; HT 31.3 ±11.6; KO 86.7 ±7.9. Average microgram of protein: WT 18.8 ±17.7; HT 22 ±9.3; 52.6 ±17.7. Bottom: Representative western blots of ApoB and ApoA-I in amniotic fluid of 12.5 d.p.c. samples. Equal amounts of total protein were loaded for each. The total amount of protein in each sample is also indicated. Fig 4.
PMID: 16301212

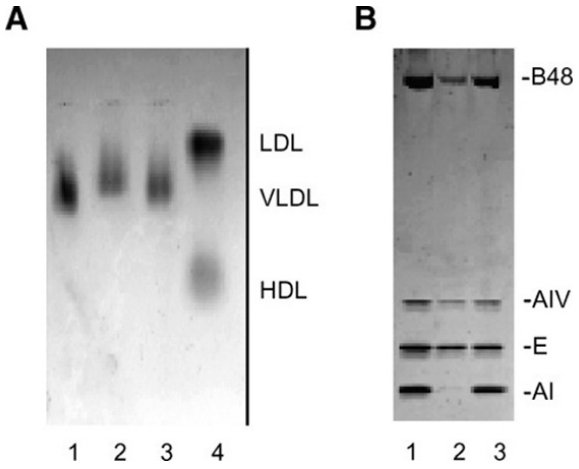

SDS-PAGE

HFD apoE4-VLDL depleted of apoA-I-rich remnants are preβ-migrating particles with similar apoE content to the original HFD VLDL. A: Agarose electrophoresis of the VLDL fraction (2.25 µg of cholesterol; lane 1), VLDL depleted of apoA-I-rich particles (2.1 µg of cholesterol; lane 2), mock depleted VLDL (2.25 µg of cholesterol; lane 3), and human plasma (4.0 µg of cholesterol; lane 4). B: SDS-PAGE electrophoresis of nonfractionated VLDL (13.5 µg of cholesterol; lane 1), VLDL depleted of apoA-I-rich particles (10.5 µg of cholesterol; lane 2), and mock depleted VLDL (13.5 µg of cholesterol; lane 3).
Fig. 4. PMID: 17264352

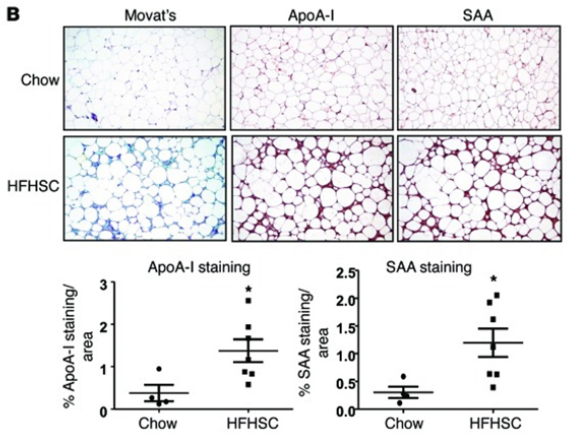

Immunohistochemistry
(B) Epididymal fat isolated from C57BL/6 mice fed chow or HFHSC diets for 20 weeks was stained with Movat's pentachrome stain and analyzed by IHC using anti–apoA-I and anti-SAA antibodies (B, n = 9). SAA colocalized with apoA-I in the ECM (blue stain with Movat's) of ATs from mice fed the HFHSC diet. Tissues were photographed using microscopy. Original magnification, ×60. Data represent mean ± SD. *P < 0.001 vs. chow. Student t test for B. Fig 7.
PMID: 26642365

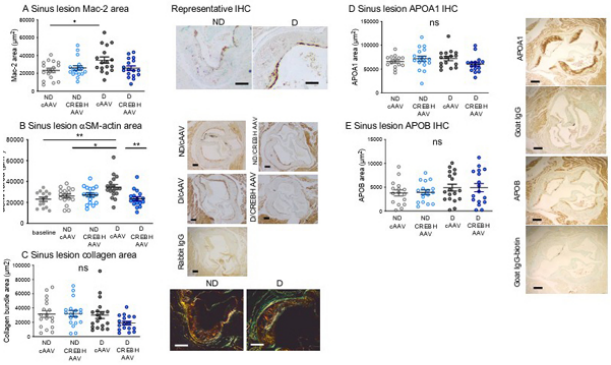

Immunohistochemistry
Diabetes increases macrophage and a-smooth muscle actin-positive cells in sinus lesions. Diabetic and non-diabetic mice expressing CREBH (CREBH AAV) or injected with a control (cAAV) were generated as described in the legend of figure 1. After 4 weeks of diabetes, mice were euthanized, and aortic sinus lesions were immunostained for Mac-2 as a marker of macrophages (A), a-smooth muscle actin as a marker of a smooth muscle cell population (B), picosirius red to evaluate collagen (C), APOA1 (D) and APOB (E). Goat IgG and Goat IgG conjugated with biotin were used for negative controls for APOA1 and APOB immunostaining, respectively. Representative images are shown. The amount of positive staining was quantified. ND, non-diabetic mice; D, diabetic mice. Mean ±SEM (n=17 ND cAAV, n=16 ND CREBH AAV, n=18 D cAAV, n=17 D CREBH AAV), ns; not significant, one-way ANOVA followed by Tukey's multiple comparisons tests. Scale bar is 100 µm. Supplemental figure 10.
PMID: 34491909

References

- Vaisar, T et al. 10,12-Conjugated linoleic acid supplementation improves HDL composition and function in mice. *Journal of Lipid Research* (2022)
- Shimizu-Albergine M et al. CREBH normalizes dyslipidemia and halts atherosclerosis in diabetes by decreasing circulating remnant lipoproteins. *J Clin Invest.* (2021)
- Han CY et al. Serum amyloid A–containing HDL binds adipocyte-derived versican and macrophage-derived biglycan, reducing its antiinflammatory properties. *JCI Insight.* (2020)
- Navdaev AV. et al. Nascent HDL (High-Density Lipoprotein) Discs Carry Cholesterol to HDL Spheres. Effects of HDL Particle Remodeling on Cholesterol Efflux. *Arteriosclerosis, Thrombosis, and Vascular Biology* (2020)
- Han et al. Serum amyloid A impairs the antiinflammatory properties of HDL. *Journal of Clinical Investigation* (2016)
- Toth ME et al. Overexpression of Hsp27 ameliorates symptoms of Alzheimer's disease in APP/PS1 mice. *Cell Stress Chaperones.* (2013)
- Fitz NF et al. Abca1 deficiency affects Alzheimer's disease-like phenotype in human ApoE4 but not in ApoE3-targeted replacement mice. *J Neurosci.* (2012)
- Champy MF et al. Reduced body weight in male Tspan8-deficient mice. *Int J Obes (Lond).* (2011)
- Tadin-Strapps M et al. siRNA-induced liver ApoB knockdown lowers serum LDL-cholesterol in a mouse model with human-like serum lipids. *J Lipid Res.* (2011)
- Dossing K et al. Apolipoprotein B epitopes are present in nuclear preparations of human and mouse cells. *Int J mol Med.* (2009)
- Cen X et al. An apoA-I mimetic peptide increases LCAT activity in mice through increasing HDL concentration. *Int J Biol Sci.* (2009)
- Hu W et al. Biogenesis of HDL by SAA is dependent on ABCA1 in the liver in vivo. *J Lipid Res.* (2008)
- Mihovilovic M et al. High-fat/high-cholesterol diet promotes a S1P receptor-mediated antiapoptotic activity for VLDL. *J Lipid Res.* (2007)
- van der Hoogt CC et al. Fenofibrate increases HDL-cholesterol by reducing cholesteryl ester transfer protein expression. *J Lipid Res.* (2007)
- de Haan W et al. Atorvastatin increases HDL cholesterol by reducing CETP expression in cholesterol-fed APOE* 3-Leiden. CETP mice. *Atherosclerosis.* (2007)
- Lefterov I et al. Expression profiling in APP23 mouse brain: inhibition of Abeta amyloidosis and inflammation in response to LXR agonist treatment. *Molecular Neurodegeneration* (2007)
- Allen E et al. Loss of polycystin-1 or polycystin-2 results in dysregulated apolipoprotein expression in murine tissues via alterations in nuclear hormone receptors. *Hum Mol Genet.* (2006)

Disclaimer

This product is for research use only and is not intended for therapeutic or diagnostic applications. Please contact a technical service representative for more information. All products of animal origin manufactured by Rockland Immunochemicals are derived from starting materials of North American origin. Collection was performed in United States Department of Agriculture (USDA) inspected facilities and all materials have been inspected and certified to be free of disease and suitable for exportation. All properties listed are typical characteristics and are not specifications. All suggestions and data are offered in good faith but without guarantee as conditions and methods of use of our products are beyond our control. All claims must be made within 30 days following the date of delivery. The prospective user must determine the suitability of our materials before adopting them on a commercial scale. Suggested uses of our products are not recommendations to use our products in violation of any patent or as a license under any patent of Rockland Immunochemicals, Inc. If you require a commercial license to use this material and do not have one, then return this material, unopened to: Rockland Inc., P.O. BOX 5199, Limerick, Pennsylvania, USA.